frontiers | Frontiers in Earth Science

TYPE Original Research
PUBLISHED 13 April 2023
DOI 10.3389/feart.2023.1060434

OPEN ACCESS

EDITED BY
Peter Varga,
ELKH Institute of Earth Physics and Space Research Seismological Observatory, Hungary

REVIEWED BY
Paolo Madonia,
Istituto Nazionale di Geofisica e Vulcanologia (INGV), Italy
Yosuke Aoki,
The University of Tokyo, Japan

*CORRESPONDENCE
S. Lambert,
sebastien.lambert@obspm.fr

SPECIALTY SECTION
This article was submitted to Solid Earth Geophysics, a section of the journal Frontiers in Earth Science

RECEIVED 03 October 2022
ACCEPTED 31 March 2023
PUBLISHED 13 April 2023

CITATION
Lambert S and Sottili G (2023), Possible role of tidal and rotational forcing on bradyseismic crises and volcanic unrest in the Campi Flegrei and Somma-Vesuvius areas.
Front. Earth Sci. 11:1060434.
doi: 10.3389/feart.2023.1060434

Possible role of tidal and rotational forcing on bradyseismic crises and volcanic unrest in the Campi Flegrei and Somma-Vesuvius areas

S. Lambert[1]* and G. Sottili[2]

[1]SYRTE, Observatoire de Paris - Université PSL, CNRS, Sorbonne Université, LNE, Paris, France, [2]Dipartimento di Scienze della Terra, Sapienza-Università di Roma, Rome, Italy

Volcanic unrest at large calderas, led by the complex interaction between the degassing of the shallow magma reservoir and the overlying hydrothermal system, occurs at intervals of 10–100 years. Even if only a minority of bradyseismic crises ends with an eruption, discriminating between pre-eruptive and non-eruptive signals is fundamental for defining levels of alert. Our study explores the possible link between recent episodes of major unrest at the Campi Flegrei caldera, located in the densely inhabited area near the city of Naples (Italy), and the astronomical forcing arising from both lunisolar tides and Earth's rotation. We analyze seismic data at Mount Vesuvius and Campi Flegrei sites and find significant correlation between the multiyear variation of the seismic energy and the tidal part of the strain, whereas the correlation with the rotational part from polar motion and length-of-day variations is more elusive. The near-zero time-lag between strain and seismicity suggests a rapid response of the seismicity to the excitation. We discuss how our findings are line with previous works evidencing how the decompression of the low-viscosity, mafic magma reservoir results in a rapid release of dissolved volatiles which in turn produces an abrupt acceleration in the Campi Flegrei caldera geochemical and geophysical signals.

KEYWORDS

bradyseism, tides, Earth's rotation, volcanic unrest, Campi Flegrei, Vesuvius

1 Introduction

Earth's rotation changes release large amounts of gravitational energy (Press and Briggs, 1975) with effects on local deformation rate (Milyukov et al., 2011), on crustal stress at a scale of the plate tectonic (Wang and Long, 2000; Riguzzi et al., 2010; Levin et al., 2013; Bendick and Bilham, 2017) and on the time-space distribution of large earthquakes (Anderson, 1958; Shanker et al., 2001; Varga et al., 2005). Concerning the effects of Earth's rotations variations on volcanoes, a causal relationship between LOD changes and occurrence of large volcanic eruptions has been proposed on a global scale at subduction margins (Palladino and Sottili, 2014; Sottili et al., 2015; Bilham et al., 2022). Also, the multi-year modulation of seismicity and eruptions magnitude by Earth's rotation axis direction variability has been detected at Mount Etna (Lambert and Sottili, 2019). The present-day scientific debate about the possible mechanism of interaction between gravitational forces and volcanism (Dumont et al., 2020;

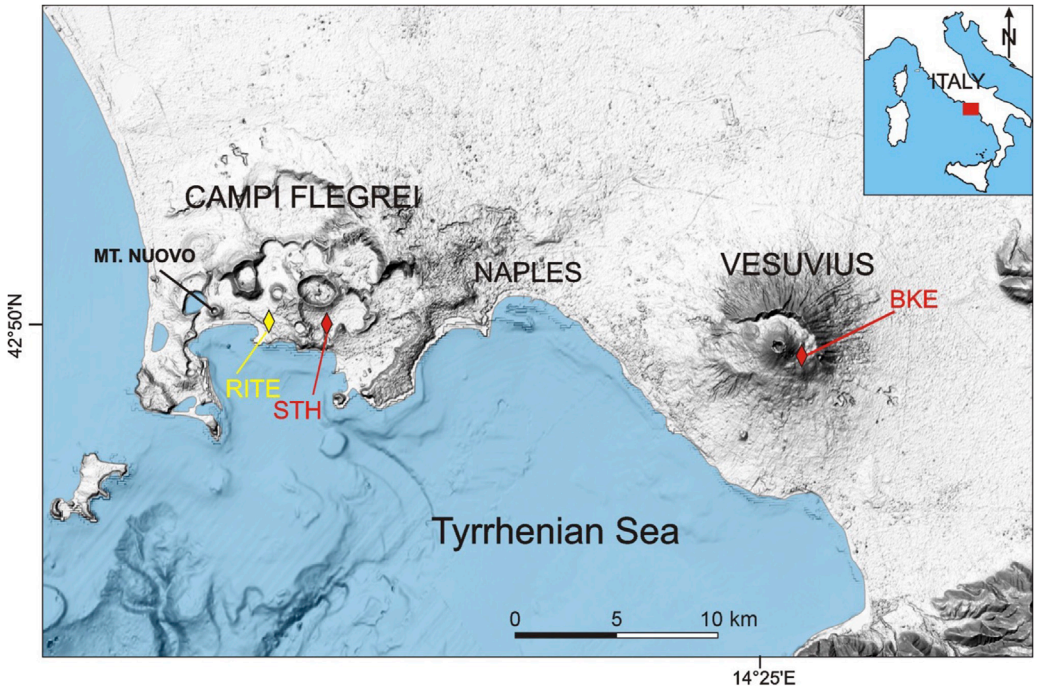

FIGURE 1
Digital Elevation Model of the Campi Flegrei and Somma-Vesuvius volcanic areas illustrating the position of the seismic and CGPS stations used in the present study. The red diamonds show the location of the Osservatorio Vesuviano - INGV seismic stations on the flanks of Somma-Vesuvius (BKE) and in the Campi Flegrei Caldera area at Pozzuoli (STH). The yellow diamond indicates the location of the RITE (Rione Terra-Pozzuoli) CGPS station where, starting from November 2005, the largest Campi Flegrei uplift was measured. The last Campi Flegrei eruption, in 1538 AD, produced the Monte Nuovo crater, which is located in the western sector of the Campi Flegrei Caldera.

2021; Sottili et al., 2021; Dumont et al., 2022) is mostly focused on the cycles of compression-decompression of wall rocks influencing the escape of magmatic volatiles (Jaggar et al., 1924; Mauk and Johnston, 1973; Connor et al., 1988; Girona et al., 2018) and promoting fluid-driven cracking of the country rocks, e.g., at Miyake-Jima (Kasahara et al., 2001) or at Stromboli (Sottili and Palladino, 2012) and decompression of shallow magma reservoirs at, e.g., Mount Etna (Sottili et al., 2007).

Concerning the role of tidal stresses on volcanism at the Campi Flegrei (CF) caldera (see **Figure 1**), a semidiurnal and quasi diurnal tidal modulation of geophysical signals from the shallow geothermal reservoir has been detected from the analysis of low-frequency events, i.e., with a main peak frequency around 0.8 Hz, and shallow seismicity (Rydelek et al., 1992; Petrosino et al., 2018). Also, tiltmetric time series analysis evidenced diurnal, fortnightly and monthly changes in the orientation and amplitude of the tilting within the caldera (De Lauro et al., 2018). Notably, tidal signals in the gravimetric and seismic time histories have been also detected during the 1982–1984 bradyseismic crisis (Berrino, 1994), whilst relatively 'drier' periods - i.e., characterized by a less intense fluids flux toward the shallow hydrothermal system - are characterized by weaker tidal signals in the geochemical and geophysical time series, as, for example, during the 2007–2010 period (Petrosino et al., 2018). This suggests a complex interaction among tidal forces, local stress field and volcano-tectonic settings superimposed to the endogenous dynamics of the CF shallow, volatile-rich hydrothermal system.

The last pre-eruptive bradyseismic crisis at the CF caldera, resulting in a net uplift of ca. 7 m, took place before the 1538 AD Monte Nuovo eruption (Bodnar et al., 2007). Since then, the area of ca. 5 km of radius from the city of Pozzuoli underwent to periodic phases of intense degassing, rapid uplift and shallow seismicity which ended with periods of slow subsidence. Typically, unrest phases are associated with important changes in the fumarolic activity and volcano-tectonic and long-period shallow seismicity, as also recorded during the ongoing unrest phase, characterized by: i) a total uplift of ca. 0.7 m in the 2005–2011 period and an increasing uplift rate since September 2020 up to ca. 10 mm per month, ii) intense fumarolic vent discharge with more than 600 tons/day of CO_2 from a single vent, iii) pressurization of the CF hydrothermal system up to ~44 bar and iv) tens of thousands shallow micro earthquakes mostly located at depths less than 4 km with more than 98% of magnitudes lower than 2.5 (D'Auria et al., 2015; Tamburello et al., 2019). The composition of volcanic gas and the geophysical signals associated to the bradyseismic crises suggest an involvement of the hydrothermal-magmatic system in the unrest phases (Chiodini et al., 2016). Specifically, the driving mechanism controlling the periodic uplift of the CF caldera, the variations of hydrothermal flux and seismicity seems to be originated by the degassing of a shallow magma reservoir transferring heat and volatiles to the overlying hydrothermal system (Chiodini et al., 2016).

This provides the theoretical background to explore the effects of Earth's rotations variations on CF bradyseismic crises which

are led by the complex interaction between the degassing of the shallow magma reservoir and the overlying hydrothermal system (Caliro et al., 2014; D'Auria et al., 2015). Here we investigate the effects of both lunisolar and centrifugal forcing, arising from Earth's rotation variations, on the magma degassing processes at the origin of bradyseismic crises at the CF caldera. We hypothesized that tidal stresses, by acting on a multiyear time scale, may enhance the supply of volatiles from portions of the [CO_2+H_2O]-saturated CF magma reservoir thus influencing the timing of bradyseismic crises occurred over the last century at the CF caldera.

2 Data and methods

This study makes use of several global and local geodetic and seismic data, the gross principal being to compare the seismic activity with the tidal forces acting on the surface. Seismic data relevant to the Neapolitan area were taken from the Osservatorio Vesuviano[1] of the Istituto Nazionale di Geofisica e Vulcanologia (INGV). They are available for two stations on the flanks of Mount Vesuvius (OVO and BKE), one station at Pozzuoli (STH), and one in Ischia island (OC9/ISC). All data sets contain epochs and magnitude of seismic events up to 31 December 2021 but starting at different epochs. While BKE data starts in 1999 and OVO data starts in 1972 with more than 10,000 events, STH data is much shorter and starts in 2007 (~3,000 events) and ISC data is sparser (145 events). Nevertheless, OVO is rather inhomogeneous and the number of recorded events along time reflects likely both the seismic activity and hardware evolution. Therefore, we focused on BKE an STH only. The time density of BKE events reveals a seismic crisis just before 2000; as a consequence, we used BKE data after 2002. The seismic energy release in time domain can be obtained from the duration magnitude M_d of the earthquakes following Richter (1961):

$$\log_{10}E = 9.9 + 1.9M_d - 0.025M_d^2, \quad (1)$$

in unit of 10^{-7} J.

Formulae transforming tidal and centrifugal potentials into strain and gravity changes are given in the Supporting Material. Tidal strain and gravity variations due to lunisolar gravitational forces at the relevant location and for periods longer than a year were obtained from the Cartwright and Tayler (1971) tide generating potential and standard values of the Love numbers (Petit and Luzum, 2010; Wahr et al., 2015). The Earth rotation contribution to the strain and the gravity was computed from polar motion and length-of-day (LOD) time series as provided by the International Earth rotation and Reference systems Service (IERS) Earth orientation parameter (EOP) product center[2], namely, the series C01 (monthly polar motion since 1846), C02 (monthly LOD since 1830). These series were elaborated by the combination of various astrometric and geodetic measurements, including optical astrometry before the 1960s and the progressive integration of space and geodetic techniques in the last quarter of the 20th century. Their precision

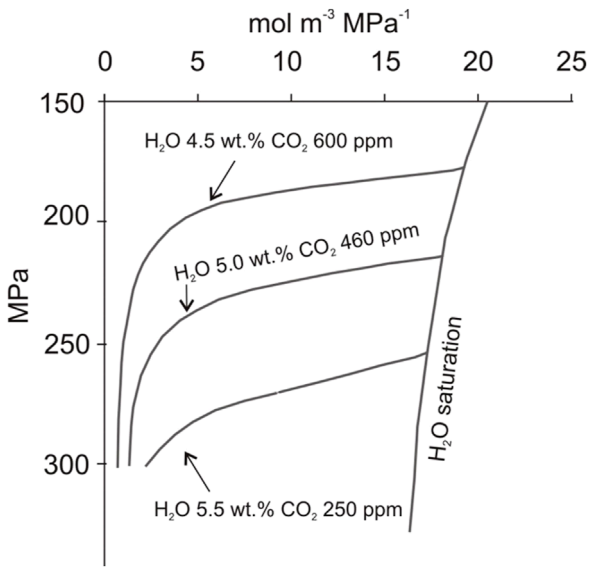

FIGURE 2
Theoretical P-X[H_2O+CO_2] degassing curves for the CF magma, calculated for 0.2 MPa decompression steps and P <300 MPa, where the mass of exsolved volatiles X[H_2O+CO_2] is expressed as moles of volatile per m^3 of trachybasaltic magma (T =1.120°C, ρ =2.650 kg m^{-3}). The plot evidences markedly different degassing styles between mixed H_2O+CO_2 vs water-bearing magmatic systems: in fact, for narrow ranges of decompression steps, the mass of volatiles released by CO_2-bearing magmatic systems increases very steeply relative to water-bearing magmatic systems.

improves from tens of centimeters in the 1920s down to less than a centimeter after 1995. As we are mainly interested in the decadal to multidecadal fluctuations rather than in the seasonal variations, we use the mean pole series provided by the IERS and representing the Gaussian low-pass filtered polar motion[3] along the entire 20th century, thereby emptied from all variations of period below ~10 years, including the Chandler and annual wobbles.

We also used ground deformation at CF from tide gauge data (1905–2009, Del Gaudio et al., 2010) completed by GNSS records of the vertical displacement of the RITE (Rione Terra, Pozzuoli) GPS station after 2000 and up to 2020 by the permanent GPS network NeVoCGPS (Neapolitan Volcanoes Continuous GPS, INGV; data were made available in De Martino et al., 2014; Bevilacqua et al., 2020; Tramelli et al., 2021).

Concerning the mechanisms controlling the cyclic bradyseismic crises at the CF caldera, these phenomena has been related to the degassing of a CO_2+H_2O saturated trachybasaltic shallow magma reservoir (Chiodini et al., 2016). We modeled quantitatively the effects of tidally induced decompression on the CF trachybasaltic magma reservoir by the VolatileCalc CO_2+H_2O solubility model (Newman and Lowenstern, 2002). We assumed isothermal conditions (T = 1,120°C) for a CO_2-H_2O saturated trachybasaltic magma reservoir at P ~200 MPa, i.e., broadly corresponding to the depth of the CF magma reservoir located at P~8 km

1 https://www.ov.ingv.it/index.php/monitoraggio-sismico-e-vulcanico-2/banche-dati.

2 https://iers.obspm.fr/eop-pc.

3 https://iers.obspm.fr/eoppc/eop/eopc01/filtered-pole.tab; https://iers.obspm.fr/eoppc/eop/eopc01/filtered-pole.readme.

depth (Cannatelli et al., 2007; Zollo et al., 2008). The intensity and compositional variations in the CF fumaroles-gas system on a multiyear scale suggest open-system conditions characterized by an efficient separation of volatiles from the magma, i.e., to each decompression step we assumed a continuous exsolution of volatiles. The open system degassing paths has been applied for 0.2 MPa decompression steps and three different initial CO_2+H_2O contents in the magma: 5.5 wt% H_2O+ 250 ppm CO_2, 5.0 wt% H_2O+ 460 ppm CO_2, 4.5 wt% H_2O+ 600 ppm CO_2. For comparison, the pure H_2O saturation curve has been also calculated (**Figure 2**).

3 Analysis and results

The seismic event series at BKE and STH are displayed in **Figure 3** where the green curves are the seismic energy release obtained by cumulating the events in bins of 6 months, illustrating the relative rest at BKE and the unrest at STH that has been linked with the accelerating bradyseismic activity and other geochemical and hydrothermal activity (Sabbarese et al., 2020). At STH, the variation of the energy released is dominated by the accelerating phase after ca. 2015 corresponding to the ongoing bradyseismic episode.

Figure 4 contains the variations of the gravity and of the components of the strain tensor induced by lunisolar tides (restrained to periods larger than a year, upper panels) and rotational effects (including polar motion and LOD variations, bottom panels) for a north latitude of 41° and an east longitude of 14° since 1900. The tidal variations are dominated at decennial periods by the lunar 18.6-year tide associated with the retrogradation of the Lunar ascending node producing a typical change in the gravity of $\delta g \sim 10^{-8}$ m/s^2 or 1 μgal. At seasonal to interannual time scales, the 'rotational tide' induced by centrifugal forcing from polar motion is mainly made up of a quasi-periodic oscillation of period about 400 days resulting from the combination of the prograde Chandler wobble (433 days) and the prograde annual wobble (365 days). Both terms, driven by atmospheric and oceanic circulation (Gross, 2000), beat and produce a modulation of the signal over a period of 6.4 years (see, e.g., Guinot, 1982), resulting in typical variations of the gravity of $\delta g \sim 2 \times 10^{-8}$ m/s^2 or 2 μgal over interannual time scales. The Chandler wobble amplitude being notably variable, the amplitude of the modulation also varies from one 6.4-year cycle to another. Over these relatively short-period effects come the aperiodic, interannual to multidecadal variations due to the long-term polar motion ('mean pole') that has been recently robustly linked to the changes in terrestrial water storage and global cryosphere (see Adhikari and Ivins, 2016). The contributions from decadal to multidecadal LOD appears to be smaller than those from the pole tide and the lunisolar tides by a factor of 5–10 and result from LOD variations attributed to torsional oscillations in the fluid outer core (Hide et al., 2000; Gillet et al., 2019).

In the following, focusing on interannual to decennial periods, all seismic energy time series were smoothed with a 4-year Loess filter to keep only the low frequency signal. To avoid edge effects consecutive to the smoothing, we removed 2 years at each bound of the series. Time series of gravity and strain variation at BKE and STH were computed at epochs of events and then binned per 3-month intervals and then treated accordingly to the seismic energy release series. The tidally-induced gravity and strain are thus reduced to the dominating 18.6-year term (and the much smaller 9.3-year term), while pole-tide and LOD-tide gravity and strain are restrained the variations observable in the third and fifth rows of the figure. Then, we computed the correlation (Spearman ρ coefficient) between the detrended series. The significance of the correlation was evaluated by testing the null hypothesis that detrended series are independent AR1 processes (Anderson, 1958) under which the sample value of the Fisher z-transformation of the correlation is expected to differ from zero by a number $s = z\sqrt{\mathrm{DOF} - 3}$ of standard deviations. Here, DOF is the number of degrees of freedom and can be estimated as the ratio of the length of the series to the length of the segment corresponding to the decorrelation time (lag for which the autocorrelation function decreases to $1/e$).

Results are shown in **Figure 5** where the correlations and the corresponding significance (Fisher's z coefficient) are reported for the optical time lag. (A positive lag corresponds to the gravity or strain variation preceding the seismic energy variation.) Considering the tidal contribution only, the gross curvature in the strain and the gravity variations reflects mainly the 18.6-year tide. At both stations, the correlation between the gravity or strain variation and the seismic energy release is significant (Fisher's z-scores of 2.3–2.5), with a good agreement in the phase of both signals in favor

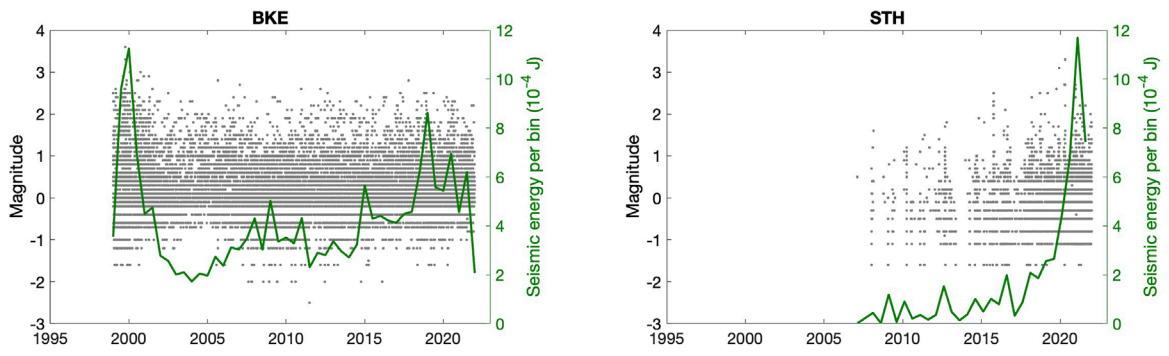

FIGURE 3
Seismic activity recorded at BKE and STH (grey dots) and time series of seismic energy release per bin of 6 months (green, solid line).

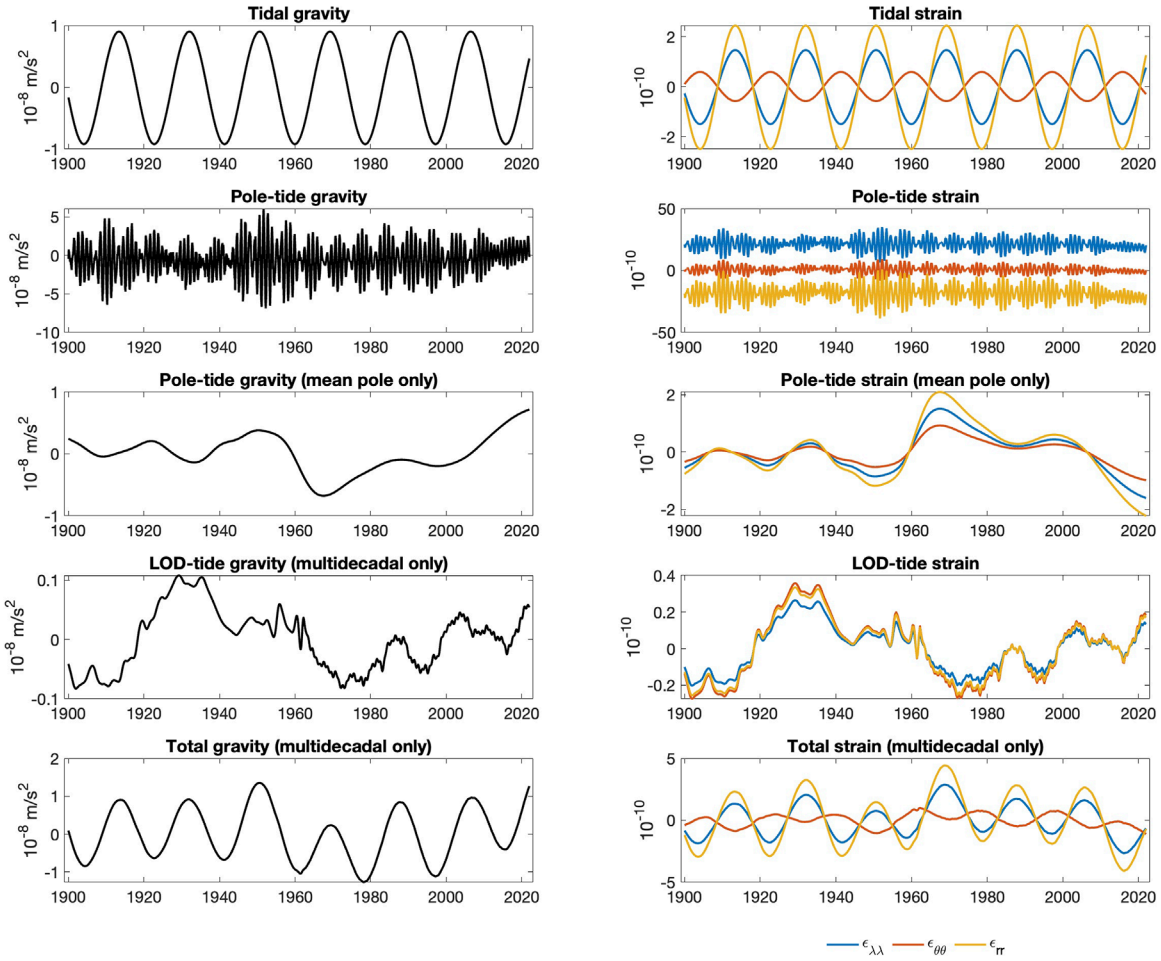

FIGURE 4
Various contributions in the variations of the tidal strain and gravity since 1900 computed for a north latitude of 41° and east longitude of 14°. In the right panels, $\epsilon_{\lambda\lambda}$ is the horizontal, eastward component of the surface strain tensor, $\epsilon_{\theta\theta}$ is the horizontal, southward component, and ϵ_{rr} is the radial (vertical) component. For readability purpose, $\epsilon_{\lambda\lambda}$ and ϵ_{rr} in the second row, right column have been shifted by 20×10^{-10} and -20×10^{-10}, respectively. As well, $\epsilon_{\lambda\lambda}$ and ϵ_{rr} in the fourth row, right column have been shifted by 0.4×10^{-10} and -0.4×10^{-10}, respectively.

of a rapid response of the seismicity to the excitation over scales of few months. Correlations are positive except for $\epsilon_{\theta\theta}$ for which the negative correlation with seismic energy is coherent with the extensional tectonic regime in the CF caldera area. In fact, since most of the CF earthquakes have similar kinematics, the computation of the stress field from focal mechanism solutions (La Rocca and Galluzzo, 2019) indicates that the σ_1 axis is vertically oriented whilst the tensile stress σ_3 is horizontal with a nearly N-S direction (i.e., 340°). In this framework, the increase of the horizontal, southward strain component determines an increase of σ_3 and, thus, a reduction of the deviatoric stress, $\sigma_1-\sigma_3$, which opposes rock failure conditions. By analogy, the positive correlation between the ϵ_{rr} vertical component and seismic energy is also consistent with the extensional tectonic regime in the CF caldera, where, to an increase of the vertical σ_1, corresponds an enhancement of the deviatoric stress, which in turn facilitates rock failure conditions. Note that at STH, the relative shortness of the seismic signal prevents one from a rigorous assessment of the correlation over a sufficiently long time period longer than the 18.6-year main tidal period.

This said, no significant correlation was found for the rotational contribution alone. The cumulation of tidal and rotational effects let unchanged the correlations between the seismic energy release and strain or gravity. If these results suggest a possible link between the tidal strain variations and the seismicity, the role of the centrifugal forcing due to Earth's polar motion and LOD variations over interannual to decadal time scales remain more elusive at this stage.

Then, we confronted the long term ground deformation at RITE with long-term tidal and rotational gravity and strain changes. A visual inspection of the elevation over the entire 20th century (in violet in **Figure 6**) suggests a concurrence between the elevation rate and the rate of the tidal/rotational forcing when the latter are lagged by 2–4 years. In order to test such possible concurrences, we separated the forcing into a positive (negative) phase defined by the time intervals of positive (negative) value of their time derivative. Then, we considered the distribution of the elevation rate during the positive and negative phases. We used a two-sided Wilcoxon rank sum test to test the significance of the difference between the medians of the distributions of elevation rates relevant to the

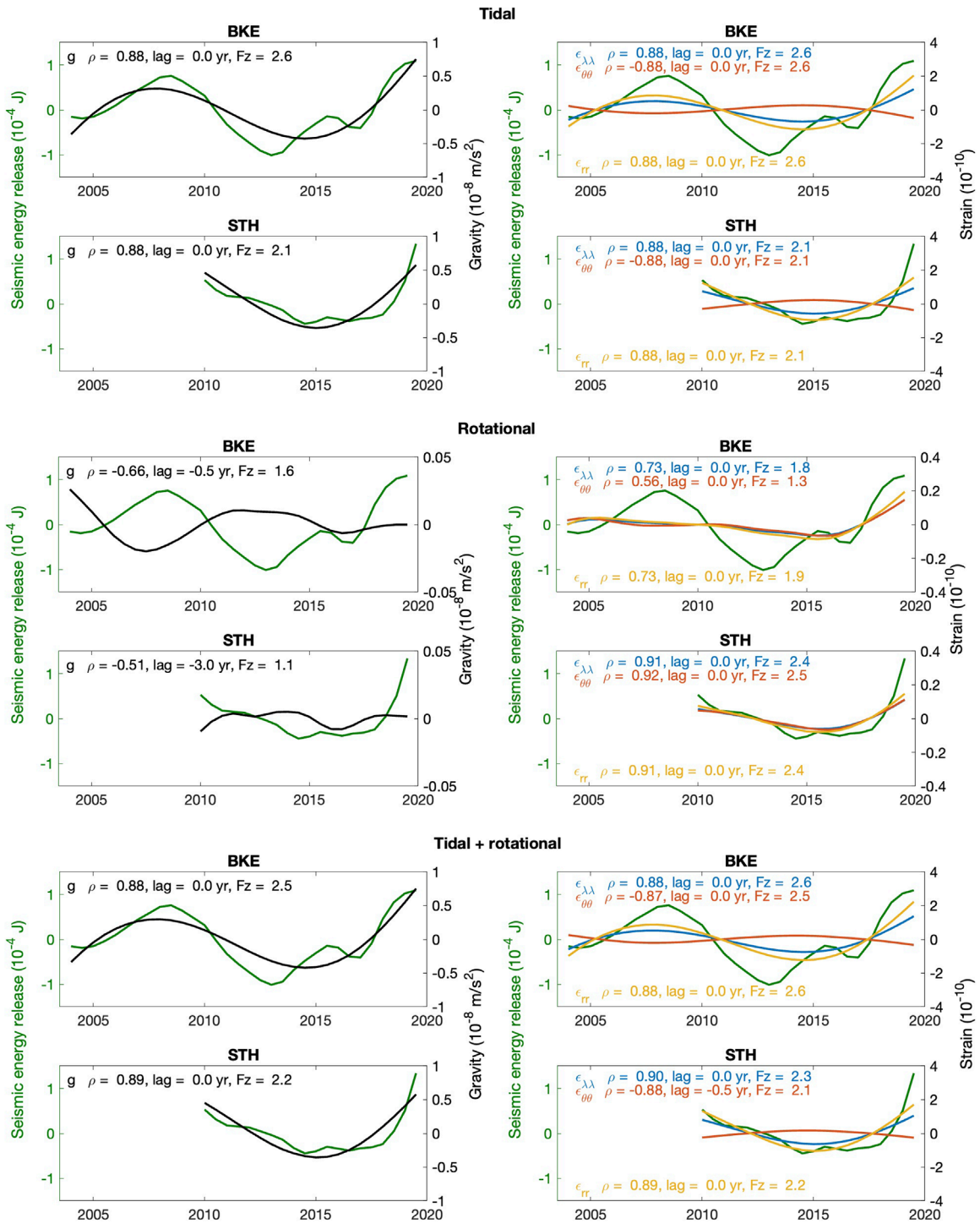

FIGURE 5
Left panels: seismic energy (in green) *versus* gravity variations (in black). Right panels: seismic energy (in green) *versus* tidal strain variations. In the right plots, $\epsilon_{\lambda\lambda}$ is the horizontal, eastward component of the surface strain tensor, $\epsilon_{\theta\theta}$ is the horizontal, southward component, and ϵ_{rr} is the radial (vertical) component. In each plot, ρ is the Spearman's coefficient and F_z the Fisher's *z* coefficient. A positive lag corresponds to the gravity or strain variation preceding the seismic energy variation.

two phases. The null hypothesis is that data in the two groups are samples from continuous distributions with equal medians. We applied several time lags within 1–10 years to the gravity and strain series with respect to the elevation data. The elevation time series is represent in **Figure 6** together with the lagged gravity and strain variations. The right panel displays whiskers of the distributions in each phase. The lags, median values and their significances are reported in **Table 1**.

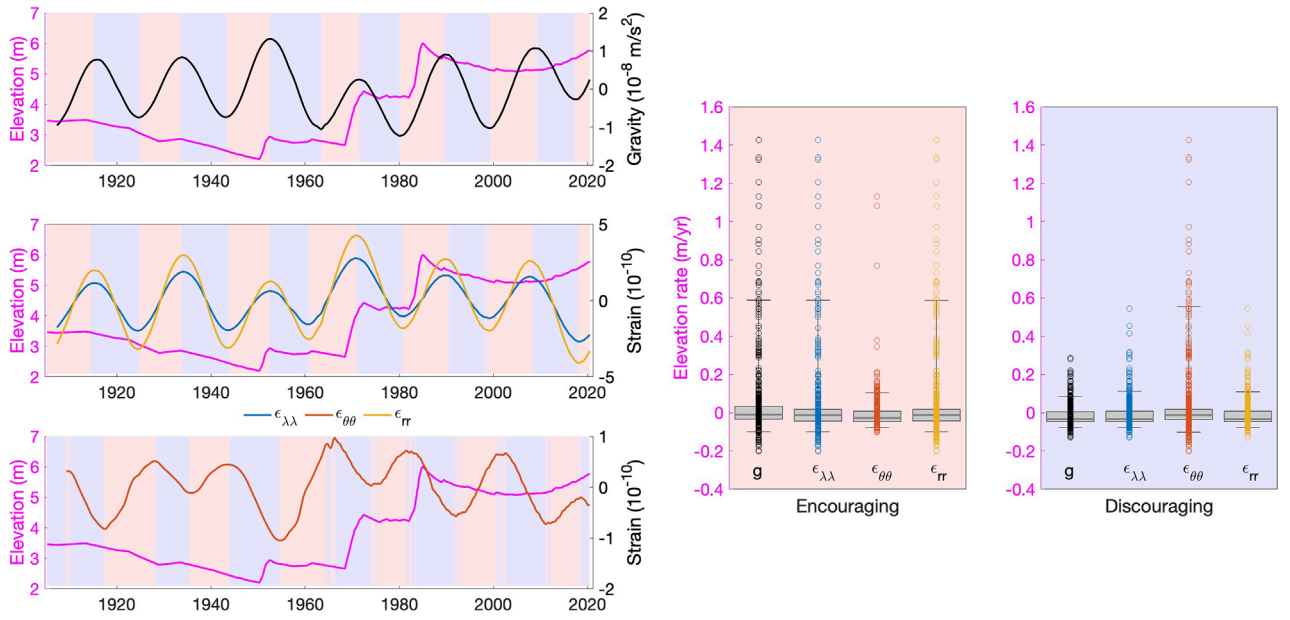

FIGURE 6
Left: comparison of the elevation (in violet) at the RITE station over the 20th century with the gravity changes and strain changes induced by lunisolar tides and Earth's rotation. The strain components are as follows: $\epsilon_{\lambda\lambda}$ is the horizontal, eastward component of the surface strain tensor, $\epsilon_{\theta\theta}$ is the horizontal, southward component, and ϵ_{rr} is the radial (vertical) component. The curves relevant to gravity, $\epsilon_{\lambda\lambda}$, and ϵ_{rr} are lagged by 2 years; the curve relevant to $\epsilon_{\theta\theta}$ is lagged by 4 years. The pink bands indicate the positive phase; the blue bands indicate the negative phases (see text for definition). Right: whisker plots of the distribution of the elevation rate in the positive and negative phases.

TABLE 1 Lag (yr) between the elevation rate and the gravity changes and strain changes, medians of the elevation rate in the positive (M_+) and negative (M_-) phases, and the associated Wilcoxon test *p*-values.

	Lag (yr)	M_+ (mm/yr)	M_- (mm/yr)	p-value
g	2	−11	−35	5×10^{-16}
$\epsilon_{\lambda\lambda}$	2	−14	−35	2×10^{-8}
$\epsilon_{\theta\theta}$	4	−28	−13	4×10^{-6}
ϵ_{rr}	2	−13	−35	8×10^{-9}

For the gravity, vertical and horizontal eastward strains, we found optimal *p*-values corresponding to extremal median differences for a lag of 2–3 years, and suggesting that the positive phase (increasing gravity and strain) encourages the elevation. In contrast, for the horizontal southward strain, the optimal *p*-values are found for lags of about 4 years with the episodes of high elevation rate concurrent with the negative phases (decreasing gravity and strain).

The above correlation studies suggest a sensitivity of geophysical and geochemical signals to the long-period (interannual to decadal) tidal forcing, and thereby a role of such forcing in controlling seismic and bradyseismic crises in the Neapolitan area. The sensitivity to the rotational forcing remains elusive on the basis of the used observational data sets and time spans. These results call for a model to identify a possible link between the tidal stresses and the physical processes controlling the caldera unrest.

The rapid acceleration of ground deformations and geochemical signals during the recent volcanic unrest, associated to an abrupt decrease of the CO_2/H_2O ratio, has been explained by the non-linear magma degassing dynamics driven by the differential solubility of H_2O and CO_2 (Chiodini et al., 2016) within a relatively shallow (i.e., ~200 MPa) magma reservoir (Buono et al., 2022).

Our results from the VolatileCalc CO_2+H_2O solubility model (Newman and Lowenstern, 2002) indicate markedly different degassing behavior for mixed CO_2+H_2O systems with respect to H_2O-system. In fact, the total amount of exsolved fluids in CO_2+H_2O mixed systems displays a strongly non-linear pressure dependence as, for P ~300 MPa, to a 1 MPa decompression step corresponds ~1 mol m^{-3} of magma whilst, at pressure <200 MPa, the mass of magmatic volatiles released per unit mass of magma increases by a factor ~20 (**Figure 2**). This means that, for P values close to the CO_2+H_2O saturation pressure, portions of the volatile saturated CF magma reservoir can be extremely sensitive to pressure perturbations by the same order of magnitude of tidal and rotational forcings (i.e., 500 Pa h^{-1}; see Lambert and Sottili, 2019). For example, at P = 200 MPa, for initial CO_2+H_2O contents in the magma of 4.5 wt% H_2O+ 600 ppm CO_2 the decompression of 500 Pa h^{-1} corresponds to ca. 100 tons per day per km^3 of magma. Overall, the relatively low solubility of volatiles in CO_2-bearing magmatic systems implies that, at P = 200 MPa, the CO_2 is completely exsolved for volatile contents by 5.0 wt% H_2O+ 460 ppm CO_2 and by 5.5 wt% H_2O+ 250 ppm CO_2 (**Figure 2**). The implications of the results from the solubility model on the tidal and

rotational forcings during CF bradyseismic crises will be discussed in the next Section.

4 Discussion

Tidally induced decompression of volcanic feeding systems, by modulating cycles of pressurization and depressurization of magma reservoirs, can lead to the exsolution of volatiles (Sottili et al., 2007) and, possibly, to a permeable volatiles flow through the upper part of volcano edifices (Girona et al., 2018; Petrosino et al., 2018). In open conduit volcanic systems, the tidally enhanced exsolution of volatiles can accelerate the transition of the volcano feeder system toward a critical state, thus influencing the timing of explosive episodes (e.g., at Stromboli and Mount Etna volcanoes; see Sottili et al., 2007; Sottili and Palladino, 2012). This 'trigger effect', as also modeled in statistical terms by Jupp et al. (2004), can occur on condition that tidal decompression rates exceed the rate of pressurization due to volcanic inner dynamics (e.g., magma cooling and crystallization; see Sottili et al., 2007). In closed conduit volcanic systems, tidal stresses can promote the permeable flow of volatiles from deeper levels toward the surface as revealed, for example, by the periodic oscillations of the amplitude of volcanic tremor (Girona et al., 2018); these oscillations of volcanic tremor has been explained by the tidally induced intermittent supply of volatiles from deeper levels, provided that the permeability of the shallow volcanic edifice is low enough (Girona et al., 2018).

At the CF caldera, the acceleration in geochemical and geophysical signals observed over the last 15 years has been related to a dramatic increase in the efficiency of heat transfer by magmatic volatiles from the deep reservoir to the overlying hydrothermal system (Sabbarese et al., 2020). On these grounds, we modeled quantitatively the effects of stress changes caused by tides and Earth rotation variations on the degassing rate from the deep magma reservoir. Specifically, the application of the CO_2+H_2O solubility model to the CF trachybasaltic magma evidences a markedly non-linear dependence of gas solubility on pressure. This implies that, to relatively small tidally induced variations of stresses (i.e., 500 Pa h^{-1}; see Lambert and Sottili, 2019) in the CO_2 saturated magma reservoir may correspond the exsolution of tens to hundreds of tons of CO_2 per day per km^3 of magma. Concerning the time scale for volatile exsolution, previous works evidenced how the decompression of the low-viscosity, mafic magma reservoir results in a rapid release of dissolved volatiles which in turn produces an abrupt acceleration in the CF caldera geochemical and geophysical signals, including seismicity and ground deformations (Woods and Cardoso, 1997; Menand and Phillips, 2007; Chiodini et al., 2016). This is in line with our findings, as the observed lack of time-lag between strain and seismicity suggests a rapid response of the seismicity to the excitation.

5 Conclusion

We suggest that the mechanisms promoting the tidal modulation of geophysical and geochemical signals during the CF bradyseismic crises is related to the effects of tidally induced decompression on nearly volatile-saturated volcanic environments. Previous works, described the effects of the external forcing on the shallow, volatile-rich CF hydrothermal system by diurnal, fortnightly and monthly tidal stresses (Rydelek et al., 1992; Berrino, 1994; De Lauro et al., 2018). These local effects are relatively more pronounced during periods of volcanic unrest, i.e., phases associated to intense fumarolic vent discharge and pressurization of the hydrothermal system (Rydelek et al., 1992; Berrino, 1994; De Lauro et al., 2018). Interestingly, this link between tidal stresses, seismic energy release and deformations is less pronounced during 'drier' period of decreased hydrothermal activity (Petrosino et al., 2018).

On the other hand, on a multiyear time-scale, we found a significant correlation between the caldera uplift rate and seismic energy release and the strain due to long-period tidal and rotational forcing. Tidal variations and changes in the velocity of the Earth's rotation can affect the state of stress in the lithosphere and its deformation fields (Riguzzi et al., 2010; Milyukov et al., 2011). These relatively large-scale, long-term effects also suggest an influence of tidal and rotational forces on crustal magma reservoirs. with significant changes in horizontal stress acting on the wall rocks of magma chambers (Sottili et al., 2015). For example, at Poas volcano where the tidally induced magma vesiculation and crystallization have been invoked to explain the periodic vertical uplift of the caldera floor (Rymer and Brown, 1989).

At the CF caldera, we modeled the effects of tidal forces in modulating the degassing rate of the CO_2+H_2O saturated trachybasaltic magma reservoir which, in turn, influence the seismic energy release and the ground deformation rate during bradyseismic crises. In the CF study case, from the application of the CO_2+H_2O solubility model, we noted a marked, non-linear dependence of gas solubility on pressure. We suggest that the low solubility of the CO_2 may explain the sensitivity of portions of the nearly saturated magma reservoir to relatively small variations of stresses.

In conclusion, the external modulation of the seismic energy release and strain due to tidal and rotational forces during the CF volcanic unrest widens the spectrum of known external forcing mechanisms influencing terrestrial volcanoes and suggests how future researches may help understand the role of non-condensable, low solubility phases in hydrothermal and magmatic systems on the sensitivity of active volcanoes to Earth's tides.

Data availability statement

Publicly available datasets were analyzed in this study. This data can be found here: https://www.ov.ingv.it/index.php/monitoraggio-sismico-e-vulcanico-2/banche-dati?id=217.

Author contributions

All authors listed have made a substantial, direct, and intellectual contribution to the work and approved it for publication.

Conflict of interest

The authors declare that the research was conducted in the absence of any commercial or financial relationships

that could be construed as a potential conflict of interest.

Publisher's note

All claims expressed in this article are solely those of the authors and do not necessarily represent those of their affiliated organizations, or those of the publisher, the editors and the reviewers. Any product that may be evaluated in this article, or claim that may be made by its manufacturer, is not guaranteed or endorsed by the publisher.

Supplementary material

The Supplementary Material for this article can be found online at: https://www.frontiersin.org/articles/10.3389/feart.2023.1060434/full#supplementary-material

References

Adhikari, S., and Ivins, E. R. (2016). Climate-driven polar motion: 2003–2015. *Sci. Adv.* 2, e1501693. doi:10.1126/sciadv.1501693

Anderson, T. W. (1958). *An introduction to multivariate statistical analysis*. Wiley.

Bendick, R., and Bilham, R. (2017). Do weak global stresses synchronize earthquakes? *Geophys. Res. Lett.* 44, 8320–8327. doi:10.1002/2017gl074934

Berrino, G. (1994). Gravity changes induced by height-mass variations at the campi flegrei caldera. *J. Volcanol. Geotherm. Res.* 61, 293–309. International Conference on Active Volcanoes and Risk Mitigation. doi:10.1016/0377-0273(94)90010-8

Bevilacqua, A., Neri, A., De Martino, P., Isaia, R., Novellino, A., Tramparulo, F. D., et al. (2020). Radial interpolation of gps and leveling data of ground deformation in a resurgent caldera: Application to Campi Flegrei (Italy). *J. Geodesy* 94, 24. doi:10.1007/s00190-020-01355-x

Bilham, R., Szeliga, W., Mencin, D., and Bendick, R. (2022). Increased caribbean seismicity and volcanism during minima in Earth's rotation rate: Search for a physical mechanism and a 2030 forecast. *Front. Earth Sci.* 10. doi:10.3389/feart.2022.1041311

Bodnar, R. J., Cannatelli, C., de Vivo, B., Lima, A., Belkin, H. E., and Milia, A. (2007). Quantitative model for magma degassing and ground deformation (bradyseism) at Campi Flegrei, Italy: Implications for future eruptions. *Geology* 35, 791. doi:10.1130/G23653A.1

Buono, G., Paonita, A., Pappalardo, L., Caliro, S., Tramelli, A., and Chiodini, G. (2022). New insights into the recent magma dynamics under Campi Flegrei caldera (Italy) from petrological and geochemical evidence. *J. Geophys. Res. Solid Earth* 127, e2021JB023773. doi:10.1029/2021JB023773

Caliro, S., Chiodini, G., and Paonita, A. (2014). Geochemical evidences of magma dynamics at Campi Flegrei (Italy). *Geochem. Cosmochim. Acta* 132, 1–15. doi:10.1016/j.gca.2014.01.021

Cannatelli, C., Lima, A., Bodnar, R. J., De Vivo, B., Webster, J. D., and Fedele, L. (2007). Geochemistry of melt inclusions from the Fondo Riccio and Minopoli 1 eruptions at Campi Flegrei (Italy). *Chem. Geol.* 237, 418–432. doi:10.1016/j.chemgeo.2006.07.012

Cartwright, D. E., and Tayler, R. J. (1971). New computations of the tide-generating potential. *Geophys. J. R. Astron. Soc.* 23, 45–73. doi:10.1111/j.1365-246x.1971.tb01803.x

Chiodini, G., Paonita, A., Aiuppa, A., Costa, A., Caliro, S., De Martino, P., et al. (2016). Magmas near the critical degassing pressure drive volcanic unrest towards a critical state. *Nat. Commun.* 7, 13712. doi:10.1038/ncomms13712

Connor, C. B., Stoiber, R. E., Malinconico, J., and Lawrence, L. (1988). Variation in sulfur dioxide emissions related to Earth tides, Halemaumau crater, Kilauea volcano, Hawaii. *J. Geophys. Res.* 93, 14867–14871. doi:10.1029/JB093iB12p14867

D'Auria, L., Pepe, S., Castaldo, R., Giudicepietro, F., Macedonio, G., Ricciolino, P., et al. (2015). Magma injection beneath the urban area of naples: A new mechanism for the 2012–2013 volcanic unrest at Campi Flegrei caldera. *Sci. Rep.* 5, 13100. doi:10.1038/srep13100

De Lauro, E., Petrosino, S., Ricco, C., Aquino, I., and Falanga, M. (2018). Medium and long period ground oscillatory pattern inferred by borehole tiltmetric data: New perspectives for the Campi Flegrei caldera crustal dynamics. *Earth Planet. Sci. Lett.* 504, 21–29. doi:10.1016/j.epsl.2018.09.039

De Martino, P., Tammaro, T., and Obrizzo, F. (2014). Gps time series at Campi Flegrei caldera (2000-2013). *Ann. Geophys.* 57. doi:10.4401/ag-6431

Del Gaudio, C., Aquino, I., Ricciardi, G. P., Ricco, C., and Scandone, R. (2010). Unrest episodes at Campi Flegrei: A reconstruction of vertical ground movements during 1905–2009. *J. Volcanol. Geotherm. Res.* 195, 48–56. doi:10.1016/j.jvolgeores.2010.05.014

Dumont, S., Le Mouël, J.-L., Courtillot, V., Lopes, F., Sigmundsson, F., Coppola, D., et al. (2020). The dynamics of a long-lasting effusive eruption modulated by Earth tides. *Earth Planet. Sci. Lett.* 536, 116145. doi:10.1016/j.epsl.2020.116145

Dumont, S., Silveira, G., Custódio, S., Lopes, F., Le Mouël, J.-L., Gouhier, M., et al. (2021). Response of Fogo volcano (Cape Verde) to lunisolar gravitational forces during the 2014–2015 eruption. *Phys. Earth Planet. Inter.* 312, 106659. doi:10.1016/j.pepi.2021.106659

Dumont, S., Petrosino, S., and Neves, M. (2022). On the link between global volcanic activity and global mean sea level. *Front. Earth Sci.* 10, 845511. doi:10.3389/feart.2022.845511

Gillet, N., Huder, L., and Aubert, J. (2019). A reduced stochastic model of core surface dynamics based on geodynamo simulations. *Geophys. J. Int.* 219, 522–539. doi:10.1093/gji/ggz313

Girona, T., Huber, C., and Caudron, C. (2018). Sensitivity to lunar cycles prior to the 2007 eruption of Ruapehu volcano. *Sci. Rep.* 8, 1476. doi:10.1038/s41598-018-19307-z

Gross, R. S. (2000). The excitation of the Chandler wobble. *Geophys. Res. Lett.* 27, 2329–2332. doi:10.1029/2000GL011450

Guinot, B. (1982). The Chandlerian nutation from 1900 to 1980. *Geophys. J. R. Astron. Soc.* 71, 295–301. doi:10.1111/j.1365-246X.1982.tb05991.x

Hide, R., Boggs, D. H., and Dickey, J. O. (2000). Angular momentum fluctuations within the Earth's liquid core and torsional oscillations of the core–mantle system. *Geophys. J. Int.* 143, 777–786. doi:10.1046/j.0956-540x.2000.01283.x

Jaggar, T. A., Finch, R. H., and Emerson, O. H. (1924). The lava tide, seasonal tilt, and the volcanic cycle. *Mon. Weather Rev.* 52, 142. doi:10.1175/1520-0493(1924)52⟨142:TLTSTA⟩2.0.CO;2

Jupp, T. E., Pyle, D. M., Mason, B. G., and Dade, W. B. (2004). A statistical model for the timing of earthquakes and volcanic eruptions influenced by periodic processes. *J. Geophys. Res. Solid Earth* 109. doi:10.1029/2003JB002584

Kasahara, J., Nakao, S., and Koketsu, K. (2001). Tidal influence on the 2000 miyake jima eruption and its implications for hydrothermal activity and volcanism. *Proc. Jpn. Acad. Ser. B* 77, 98–103. doi:10.2183/pjab.77.98

La Rocca, M., and Galluzzo, D. (2019). Focal mechanisms of recent seismicity at Campi Flegrei, Italy. *J. Volcanol. Geotherm. Res.* 388, 106687. doi:10.1016/j.jvolgeores.2019.106687

Lambert, S., and Sottili, G. (2019). Is there an influence of the pole tide on volcanism? Insights from Mount Etna recent activity. *Geophys. Res. Lett.* 46, 13730–13736. doi:10.1029/2019GL085525

Levin, B., Domanski, A., and Sasorova, E. (2013). Zonal concentration of some geophysical process intensity caused by tides and variations in the Earth's rotation velocity. *Adv. Geosci.* 35, 137–144. doi:10.5194/adgeo-35-137-2014

Mauk, F. J., and Johnston, M. J. S. (1973). On the triggering of volcanic eruptions by Earth tides. *J. Geophys. Res.* 78, 3356–3362. doi:10.1029/JB078i017p03356

Menand, T., and Phillips, J. C. (2007). Gas segregation in dykes and sills. *J. Volcanol. Geotherm. Res.* 159, 393–408. doi:10.1016/j.jvolgeores.2006.08.003

Milyukov, V. K., Kravchyuk, V. K., Mironov, A. P., and Latynina, L. A. (2011). Deformation processes in the lithosphere related to the nonuniformity of the Earth's rotation. *Izvestiya, Phys. Solid Earth* 47, 246–258. doi:10.1134/S1069351311020042

Newman, S., and Lowenstern, J. B. (2002). Volatilecalc: A silicate melt–H2O–CO2 solution model written in visual basic for excel. *Comput. Geosci.* 28, 597–604. doi:10.1016/S0098-3004(01)00081-4

Palladino, D. M., and Sottili, G. (2014). Earth's spin and volcanic eruptions: Evidence for mutual cause-and-effect interactions? *Terra Nova.* 26, 78–84. doi:10.1111/ter.12073

Petit, G., and Luzum, B. (2010). *IERS technical note 36: IERS conventions 2010*. Tech. rep. Bundesamts für Kartographie und Geodäsie.

Petrosino, S., Cusano, P., and Madonia, P. (2018). Tidal and hydrological periodicities of seismicity reveal new risk scenarios at Campi Flegrei caldera. *Sci. Rep.* 8, 13808. doi:10.1038/s41598-018-31760-4

Press, F., and Briggs, P. (1975). Chandler wobble, earthquakes, rotation, and geomagnetic changes. *Nature* 256, 270–273. doi:10.1038/256270a0

Richter, C. F. (1961). Elementary seismology. *Geol. J.* 2, xi–xiii. doi:10.1002/gj.3350020212

Riguzzi, F., Panza, G., Varga, P., and Doglioni, C. (2010). Can Earth's rotation and tidal despinning drive plate tectonics? *Tectonophysics* 484, 60–73. Quantitative modelling of geological processes. doi:10.1016/j.tecto.2009.06.012

Rydelek, P. A., Sacks, I. S., and Scarpa, R. (1992). On tidal triggering of earthquakes at Campi Flegrei, Italy. *Geophys. J. Int.* 109, 125–135. doi:10.1111/j.1365-246X.1992.tb00083.x

Rymer, H., and Brown, G. (1989). Gravity changes as a precursor to volcanic eruption at Poás volcano, Costa Rica. *Nature* 342, 902–905. doi:10.1038/342902a0

Sabbarese, C., Ambrosino, F., Chiodini, G., Giudicepietro, F., Macedonio, G., Caliro, S., et al. (2020). Continuous radon monitoring during seven years of volcanic unrest at Campi Flegrei caldera (Italy). *Sci. Rep.* 10, 9551. doi:10.1038/s41598-020-66590-w

Shanker, D., Kapur, N., and Singh, V. P. (2001). On the spatio temporal distribution of global seismicity and rotation of the Earth —A review. *Acta Geod. Geophys. Hung.* 36, 175–187. doi:10.1556/AGeod.36.2001.2.5

Sottili, G., and Palladino, D. M. (2012). Tidal modulation of eruptive activity at open-vent volcanoes: Evidence from Stromboli. *Terra Nova.* 24, 233–237. doi:10.1111/j.1365-3121.2012.01059.x

Sottili, G., Martino, S., Palladino, D. M., Paciello, A., and Bozzano, F. (2007). Effects of tidal stresses on volcanic activity at Mount Etna, Italy. *Geophys. Res. Lett.* 34, L01311. doi:10.1029/2006GL028190

Sottili, G., Palladino, D. M., Cuffaro, M., and Doglioni, C. (2015). Earth's rotation variability triggers explosive eruptions in subduction zones. *Earth, Planets Space* 67, 208–209. doi:10.1186/s40623-015-0375-z

Sottili, G., Lambert, S., and Palladino, D. M. (2021). Tides and volcanoes: A historical perspective. *Front. Earth Sci.* 9, 1261. doi:10.3389/feart.2021.777548

Tamburello, G., Caliro, S., Chiodini, G., De Martino, P., Avino, R., Minopoli, C., et al. (2019). Escalating CO2 degassing at the Pisciarelli fumarolic system, and implications for the ongoing Campi Flegrei unrest. *J. Volcanol. Geotherm. Res.* 384, 151–157. doi:10.1016/j.jvolgeores.2019.07.005

Tramelli, A., Godano, C., Ricciolino, P., Giudicepietro, F., Caliro, S., Orazi, M., et al. (2021). Statistics of seismicity to investigate the Campi Flegrei caldera unrest. *Sci. Rep.* 11, 7211. doi:10.1038/s41598-021-86506-6

Varga, P., Gambis, D., Gráczer, Z., and Bizouard, C. (2005). "The relationship between the global seismicity and the rotation of the Earth," in Journées 2005 Systèmes de Références Spatio-Temporels, 115–120.

Wahr, J., Nerem, R. S., and Bettadpur, S. V. (2015). The pole tide and its effect on grace time-variable gravity measurements: Implications for estimates of surface mass variations. *J. Geophys. Res. Solid Earth* 120, 4597–4615. doi:10.1002/2015JB011986

Wang, S., and Long, X. (2000). Study on tectonic stress field in Tengchong. *J. Seismol. Res.* 23, 172–178.

Woods, A. W., and Cardoso, S. S. S. (1997). Triggering basaltic volcanic eruptions by bubble-melt separation. *Nature* 385, 518–520. doi:10.1038/385518a0

Zollo, A., Maercklin, N., Vassallo, M., Dello Iacono, D., Virieux, J., and Gasparini, P. (2008). Seismic reflections reveal a massive melt layer feeding Campi Flegrei caldera. *Geophys. Res. Lett.* 35, L12306. doi:10.1029/2008GL034242